Journal of Cellular Biochemistry 99:435–449 (2006)

Reduction of Anabolic Signals and Alteration of Osteoblast Nuclear Morphology in Microgravity

Millie Hughes-Fulford,[1,2,3]* Karsten Rodenacker,[4] and Uta Jütting[4]

[1]Northern California Institute for Research and Education, San Francisco, California
[2]Department of Medicine, University of California, San Francisco, California
[3]Department of Veteran Affairs, Laboratory of Cell Growth and Differentiation, San Francisco, California
[4]GSF—National Research Center for Environment and Health, Institute of Biomathematics and Biometry, Ingolstädter Landstraße 1, D-85764 Neuherberg, Germany

Abstract Bone loss has been repeatedly documented in astronauts after flight, yet little is known about the mechanism of bone loss in space flight. Osteoblasts were activated during space flight in microgravity (μg) with and without a 1 gravity (1 g) field and 24 genes were analyzed for early induction. Induction of *proliferating cell nuclear antigen (PCNA), transforming growth factor β (TGFβ), cyclo-oxygenase-2 (cox-2), cpla2, osteocalcin (OC), c-myc, fibroblast growth factor-2 (fgf-2), bcl2, bax,* and *fgf-2* message as well as FGF-2 protein were significantly depressed in μg when compared to ground (gr). Artificial onboard gravity normalized the induction of *c-myc*, *cox-2*, *TGFβ*, *bax*, *bcl2*, and *fgf-2* message as well as FGF-2 protein synthesis in spaceflight samples. In normal gravity, FGF-2 induces *bcl2* expression; we found that *bcl2* expression was significantly reduced in microgravity conditions. Since nuclear shape is known to elongate in the absence of mitogens like FGF-2, we used high-resolution image-based morphometry to characterize changes in osteoblast nuclear architecture under microgravity, 1 g flight, and ground conditions. Besides changes in cell shape (roundish/elliptic), other high-resolution analyses show clear influences of gravity on the inner nuclear structure. These changes occur in the texture, arrangement, and contrast of nuclear particles and mathematical modeling defines the single cell classification of the osteoblasts. Changes in nuclear structure were evident as early as 24 h after exposure to microgravity. This documented alteration in nuclear architecture may be a direct result of decreased expression of autocrine and cell cycle genes, suggesting an inhibition of anabolic response in μg. Life on this planet has evolved in a normal gravity field and these data suggest that gravity plays a significant role in regulation of osteoblast transcription. J. Cell. Biochem. 99: 435–449, 2006.

Key words: microgravity; growth regulation; cytometry; morphometry; photometry; *fgf*-2; *bcl*2

A projected bone loss of 20–30% in astronauts is one of the major physiological show stoppers in the proposed 30-month manned mission to Mars. For the first three decades of space flight, scientists have discovered systemic changes in the body, which included loss of bone and increases in urinary calcium. From these animal and human studies, investigators found that loss of weight bearing bone can be as high as 3% per month and this loss is primarily due to lack of new osteoblast growth in space flight [Wronski and Morey, 1983; Nicogossian et al., 1989; Marie et al., 2000; Vico et al., 2000]. Although flight opportunities have been limited, the volume of data about microgravity effects on cell proliferation and differentiation is accumulating. It has been demonstrated that cell growth and differentiation of osteoblasts is inhibited or altered in a microgravity environment [Fitzgerald and Hughes-Fulford, 1996; Hughes-Fulford and Lewis, 1996; Carmeliet et al., 1998; Landis et al., 2000; Granet et al., 2001] suggesting that the osteoporosis seen in spaceflight is occurring at the cellular level. Altered gene expression, reduction in transcription factors, and reductions in growth factor

Grant sponsor: NASA; Grant numbers: NAG-2-1086, NAG-2-1286, NCC-2-136; Grant sponsor: Department of Veterans Affairs Research Service Merit Review.

*Correspondence to: Millie Hughes-Fulford, PhD, Director, Lab of Cell Growth, VA Medical Center Mail Code 151F, 4150 Clement Street, San Francisco, CA 94121.
E-mail: milliehf@aol.com

Received 12 January 2006; Accepted 15 February 2006
DOI 10.1002/jcb.20883

related proteins have also been observed in other cells in microgravity [de Groot et al., 1990; Cubano and Lewis, 2000; Goodwin et al., 2000]. In 2001, Lewis et al. found a 5.9-fold reduction in message for TGFα in space-flown lymphocytes [Lewis et al., 2001].

In this report, we found significant reduction in expression of several osteoblast genes including fibroblast growth factor-2 (*fgf-2*), cyclo-oxygenase-2 (*cox-2*), *c-myc*, transforming growth factor β (*TGFβ*), proliferating cell nuclear antigen *(PCNA*), *osteocalcin* (OC), and *bax* in osteoblasts grown in μg. Since *fgf-2*, *TGFβ*, and *cox-2* are osteoblast autocrine/paracrine factors important in the G1-S phase transition [Canalis et al., 1991; Hughes-Fulford et al., 1992; Stachowiak et al., 1994; Coffin et al., 1995; Keresztes and Boonstra, 1999], it is possible that their decreased expression might be linked with inhibition of activation of bone growth in microgravity.

Since *fgf-2* is a known osteoblast autocrine/paracrine factor important in the G1-S phase transition [Canalis et al., 1991; Stachowiak et al., 1994; Coffin et al., 1995; Keresztes and Boonstra, 1999], we hypothesized that changes in *fgf-2* expression may be linked to inhibition of bone growth in μg. In this study, two groups of osteoblasts onboard the Space Shuttle were exposed to μg for 19 h before they were stimulated with fetal calf sera (FCS); one group was grown in microgravity, the other in an artificial 1 g environment. We analyzed expression of *fgf-2*, a mitogen, and transcription factor that promotes proliferation.

As part of our study of *fgf-2* induction, we examined concomitant changes in nuclear morphology of osteoblasts grown in microgravity. Rijken [de Groot et al., 1991] first noticed changes in cell shape in response to changed gravity in sounding rocket experiments in 1991. Morphologic changes were also reported in parabolic flight with osteoblasts exhibiting cytoplasmic retraction and membrane ruffling in ROS/17/2.8 cells [Guignandon et al., 1995]. Increased PGE_2 was also found in media, accompanied by significant flight-induced changes that included a decrease in cell area and irregular shape in some cells [Guignandon et al., 1995]. Indomethacin reduced the irregular shape changes, but not the loss of cell area. Osteoblasts grown in microgravity on STS-56 demonstrated a reduction of growth in osteoblasts activated in-flight, suggesting that microgravity caused a decrease in cell proliferation resulting in changes in cytoskeleton. A portion of the cells exhibited a spindle shape after 4 days in microgravity, with the most dramatic change observed being the elongation of nuclear shape [Fitzgerald and Hughes-Fulford, 1996].

Since it has been suggested that changes in nuclear architecture and control of gene expression are interrelated [Debnath et al., 1999], we analyzed message expression of other genes involved in cell growth and correlated morphological changes between osteoblasts grown in microgravity, 1 g or gr. In this study we report significant microgravity-induced alterations in transcription factor message and protein expression accompanied by dramatic changes in osteoblast cell morphology. The changes in gene expression observed in osteoblasts in μg were not observed in osteoblasts maintained in an in-flight 1 g field, implying a gravity requirement for normal osteoblast growth. These combined changes in osteoblast cell physiology suggest that the decrease in bone formation in astronauts may be in part due to microgravity-induced alterations in the osteoblast at the gene expression and signal transduction level.

MATERIALS AND METHODS

Preparation of Cells

The MC3T3-E1 osteoblast cell line clonally derived from embryonic mouse calvaria [Hiramatsu et al., 1983], was kindly provided to us by Dr. M. Kumegawa (Josai Dental University, Japan). The cell line was maintained at low passage number. Cells were grown in alpha minimal essential medium (αMEM) with 10% fetal calf serum (Hyclone Labs, Inc., Logan, UT) supplemented with 2 mM L-glutamine (Sigma, St. Louis, MO), 25 mM HEPES, and antibiotic–antimycotic solution (100 U penicillin/ml, 0.01 mg streptomycin/ml, 0.25 mg amphotericin B/ml). Cells were grown in a 37°C incubator with 5% CO_2. They were fed three times a week and passaged at confluence. For spaceflight experimental samples, 120,000–200,000 cells were plated onto non-coated, sterile 11×22 mm glass coverslips (Thomas Scientific, Swedesboro, NJ), placed in 6-well plates, and grown in 10% serum-containing αMEM overnight. Cell-coated coverslips were then transferred into 2% serum-containing medium for spaceflight in plungerbox units. In accordance with NASA flight rules, the plungerbox units were held for 17 h in the Shuttle at

mid-deck temperature prior to launch. This, combined with low serum-containing medium, placed the osteoblast in a quiescent state prior to Space Shuttle launch. In order to achieve our goal to study changes in nuclear morphology in microgravity, we launched cells in a quiescent condition. Osteoblasts were sera activated on-orbit and μg or 1 g samples collected in-flight (Fig. 1). There were four samples (n = 4) for each time point in μg, 1 g flight, and gr samples. NASA's LSLE (Life Sciences Laboratory Equipment) freezer, was used for sample storage on the Space Shuttle. Supplements, such as dexamethasone β-glycerol phosphate and ascorbic acid were not added to the media since these agents are known to directly effect gene expression and cell morphology of the osteoblast.

Biorack Facility and Osteo Hardware

Cells were grown in the Biorack, a multiuser facility, which consists of incubators with variable gravity centrifuges, a cooler, a freezer, and a sealed glovebox. Two identical Biorack modules were used: one remained on earth (gr samples) and the other was integrated into SpaceHab and flown on each of the Space Shuttle flights STS-76, STS-81, and STS-84. Biorack has an important advantage over other microgravity facilities in that it provides a small radius (78 mm), slow rotating (107.0 ± 0.5 rpm) centrifuge for artificial 1 g in orbit. Because of their proximity, both the μg and 1 g samples experience identical launch vibrations, accelerations, cosmic radiation, and other unknown conditions of flight. In addition, an identical experiment was performed in the Biorack module on earth gr samples with a 2 h delay from in-flight procedures in order to control for any off-nominal operations during the flight. The Osteo (the name of this flight experiment) spaceflight hardware was designed according to European Space Agency (ESA) specifications for use in the Biorack facility and constructed by

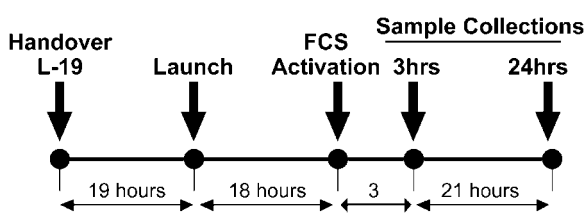

Fig. 1. Time line of experiment from handover. 19 h prelaunch, activation in-flight, and termination of experiment in-flight.

Centrum voor Constructie Mechatronica (CCM; Neuenen, Netherlands). The hardware consisted of the CCM plungerbox and its Type I container developed for spaceflight cell culture. The Type I container provided a second level of fluid containment. The plungerboxes were designed to provide a sterile environment for cell growth activation and fixation in a microgravity condition. The plungerbox is composed of two independent culture chambers that each hold two 11 mm × 22 mm glass coverslips. Each culture chamber was a separate sample. For each condition a sample size of n = 4 independent cultures was used. Each separate culture chamber has a series of reservoirs filled by either 10% serum-containing αMEM or fixative, which can be transferred into and out of the cell culture compartment by manually releasing a spring-loaded plunger.

Experiment Time Line

Quiescent cells were stored in the Space Shuttle mid-deck locker until 19 h after launch. The astronauts then transferred the samples into a 37°C incubator for 1 h before stimulating the cells to grow in the 1*g* centrifuge or μg static rack by changing their media from 2% serum to 10% serum-containing medium (T = 0). μg and 1 g samples were fixed during flight at 24 h with 3.7% formaldehyde solution and were stored at +5°C for the remainder of the Space Shuttle mission, while the GITC samples were frozen until return. There were four separate independent samples for each gravity condition at each time point (Fig. 1).

BIOCHEMICAL MEASUREMENTS

FGF-2 Protein Analysis

Analysis of FGF-2 was completed with a Quantities ELISA Immunoassay (R&D Systems, Inc., Minneapolis, MN) according to manufacturer's instructions. Cellular protein was collected from the GITC subnatant as previously described [Fitzgerald and Hughes-Fulford, 1999].

Analysis of Gene Expression

Table I shows the overview of gene expression measured in these experiments. RNA was extracted and purified by a modified acid guanidium thiocyanate/phenol/chloroform extraction method previously described [Fitzgerald and Hughes-Fulford, 1996; Barry et al., 1999; Fitzgerald and Hughes-Fulford, 1999].

TABLE I. Osteoblast Gene Expression in Microgravity

GENE	STS-76, 81, and 84 composite			
	Time point	# Of cycles	Present	Significant change
18s	T = 0	18	Yes	No
	T = 3	18	Yes	
	T = 24	18	Yes	
CPHI	T = 0	22	Yes	No
	T = 3	24	Yes	
	T = 24	24	Yes	
IL-1a	T = 0	42	No	—
	T = 3	42	No	
	T = 24	42	No	
cox-2	T = 0	34	Yes	Yes
	T = 3	30	Yes	
	T = 24	30	Yes	
cox-1	T = 0	40	No	—
	T = 3	40	No	
	T = 24	40	No	
cpla2	T = 0	32	Yes	Yes
	T = 3	32	Yes	
	T = 24	32	No	
EP1	T = 0	37	Yes	No
	T = 3	37	Yes	
	T = 24	37	Yes	
EP2	T = 0	40	No	—
	T = 3	40	No	
	T = 24	40	No	
EP3	T = 0		—	—
	T = 3	47	No	
	T = 24	47	No	
LDLr	T = 0	38	—	—
	T = 3	38	No	
	T = 24	38	No	
Cyclin A	T = 0	38	Yes	No
	T = 3	38	Yes	
	T = 24	38	Yes	
Cyclin E	T = 0	38	—	No
	T = 3	38	Yes	
	T = 24	38	Yes	
PCNA	T = 0	42	Yes	No
	T = 3	42	Yes	
	T = 24	42	—	
c-myc	T = 0	38	Yes	Yes
	T = 3	38	Yes	
	T = 24	38	Yes	
cjun	T = 0	35	No	—
	T = 3	35	No	
	T = 24	35	No	
TGFβ1	T = 0	38	Faint	Yes
	T = 3	38	Yes	
	T = 24	38	No	
FGF-2	T = 0	34	—	Yes
	T = 3	34	No	
	T = 24	34	Yes	
Actin	T = 0	30	Yes	No
	T = 3	30	Yes	
	T = 24	30	Yes	
Fibronectin	T = 0	34	Yes	No
	T = 3	34	Yes	
	T = 24	34	Yes	
Collagen	T = 0	33	No	—
	T = 3	33	No	
	T = 24	33	No	
Osteocalcin	T = 0		—	Yes
	T = 3	38	Yes	
	T = 24	38	Yes	
β1 *integrin*	T = 0	47	No	—
	T = 3	47	No	
	T = 24	47	No	
Bax	T = 0	30	Yes	Yes
	T = 3	30	Yes	
	T = 24	30	Yes	
bcl2	T = 0	34	Yes	Yes
	T = 3	38	Yes	
	T = 24	38	Yes	

Osteoblasts were flown on the Shuttle in a quiescent state; after insertion into orbit, the cultures were activated with FCS. Many of the genes that had significantly changed expression in microgravity are early pleiotopic genes that normally are increased by growth factors found in FCS. Significant changes at the collection timepoints (Fig. 1) are seen in Figures 2 and 3 (n = 4).

RT-PCR Analysis

The semi-quantitative RT-PCR analysis and primer sequences for many of the genes have been described [Fitzgerald and Hughes-Fulford, 1996; Barry et al., 1999; Fitzgerald and Hughes-Fulford, 1999]. To correct for small variations between experiments, each PCR product was compared to an internal standard of cyclophilin or 18 S products derived from the same RT reaction. Since sample size was small (200,000 cells), RNA content was held constant and linear RT-PCR was accomplished by varying the number of PCR cycles. Primers were designed in this laboratory to span introns to eliminate the possibility of detection of DNA. PCR conditions were established so that amplification reaction was stopped in the linear range. Primers not previously described are **18s** F-TCA AGA ACG AAA GTC GGA GG; R-GGA CAT CTA AGG GCA TCA CA; **CPHI** F-CGT CTC CTT TGAG CTG TTT GCA GAC R-CAT AAT CAT AAA C TAA CTC TGC AAT CCA GC; **fgf-2** F-AAC TAC AAC TTC AAG CAG AAG AGA GAR-TTA AGA TCA GCT CTT AGC AGA CAT; **bcl2** F ACTTGTG GCCCA GATAGG-CACCCAG; R CGACTTC GCCGAGATG TCCAGC CAG; **IL-1β** F-GTC TCT GAA TCA GAA ATC CTT CTA TC **R**-ATG TCA AAT TTC ACT GCT TCA TCC; **cpla2** F-GGA TTC TCT GGT GTG ATG AAG G, **R**-CCC AAT CTG CAA ACA TCA GC **ep1** F-CTG GAG GGG CGT GTC ATT TC, R- GCT GCG GAG GGT GGC TGT GG **ep2** F-CTA CGC CGC CTT CTC TTA CAT G, R-GAT GTC TTT CAC CAC GTT TGG C; **ep3** CAT CAC CAT GAT GGT CAC TGG C, R-GTC TTC ATG TGG CTG GGA TAC C; **LDLr** F-CAA TGT CTC ACC AAG CTC T, R-TCT GTC TCG AGG GGT AGC T; **cyclin A** F AAA CAG CCT GCC TTC ACC ATT CA R-ATA TTC TTC TCC CAC CTC AAC CA; **cyclin E**, F-CAA GTG GCC TAT GTC AAC GA R- ACT GCT GGG TGG GGG TGT CA; **PCNA** F-CAC CAA ATC AAG AGA AAG TT, R-GAG AAT GGA GAG AAA AGA AA; **c-myc** F-CCA ACA GGA ACT ATG ACC TCG, R-CCA CAT ACA GTC CTG GAT G; **cjun** F-GGA AAC GAC CTT CTA TGA CGA TGC CCT CAA, R-GAA CCC CTC CTF CTC ATC TGT CAC GTT CTT; **collagen**, F-GTC CCC CTG GCT CTG CTG GTT, R- TTT GGG TTG TTC GTC TGT TTC; **β1 Integrin**, TGT TCA GTG CAG CCT TCA, R-CCT CAT ACT TCG GAT TGA CC; **bax** F-CAG CTC TGA GCA GAT CAT GAA GAC A, R-GCC CAT CTT CTT CCA GAT GGT GAG C.

Cell Morphology

Osteoblasts were fixed on coverslips with 3.7% formaldehyde in phosphate buffered saline during spaceflight and stored at 5°C for 1–2 weeks before staining. There was no visible difference between control samples that were immediately stained and samples stored in formaldehyde at 5°C. For nuclear visualization, coverslips were stained with Hoechst dye number 33258 and rinsed in distilled water. The dried osteoblast coverslips were mounted onto slides and photographed with a Zeiss Axioscope microscope at 40× and 100× magnification. Slides were processed at the same time under identical conditions. Photographic exposure was taken at identical exposure times and conditions (Tables VI and VII; Figs. 4–7, 9).

IMAGING METHODS

Image Acquisition

Table II shows number of images at the total number of cells evaluated. Images were digitized from the color film slides with an Epson Expression 836XL scanner into Adobe Photoshop (Adobe Systems, Inc., Mountain View, CA) (Table III and Fig. 4). Images were stored as RGB (red, green, blue) TIF format image files (Fig. 5). From these RGB images (Fig. 5a) only the RED channel image (Fig. 5R) was used since the nuclear structure is best represented by this channel.

Image Preprocessing and Segmentation

All image analysis was performed with IDL software (Interactive Data Language, Research System, Inc., Boulder, CO). For segmentation, a global luminance value was automatically estimated from every image L and used for thresholding of the image content into background and rough cell nuclei mask M_r (Fig. 6). Cell cluster consisting of touching or occluding cells were delineated by manual interaction. Border touching cells were deleted resulting in mask M. The

TABLE II. Number of Images and Cells Evaluated

Abbreviation	Number of images	Number of cells	Description
gr	3	62	Normal gravity
1 g (flight)	5	88	Gravity by centrifuge
μg (flight)	3	52	Static in flight

TABLE III. Three-Class Jackknifed Classification Results With the Four Most Important Features and Their Corresponding *F*-Values (Also see Table VI)

	%	gr	1 g	μg	Feature	*F*-value
gr	75	47	13	2	P2A	49.7
1 g	58.0	22	51	15	HETERO	28.4
μg	88.5	1	5	46	GCV	22.7
Total	71.3				RHA	11.3

cutting lines for the edge of touching cells were set in the center of the overlapping or occluding, typically lens-shaped areas. Nuclei with large overlap with others were rejected from further analysis. For feature extraction, the RED channel, image R (Fig. 5R) was transformed to the fluorescence density image F (Fig. 5c) by the formula:

$$F = -\log\frac{255 - R}{\max(255 - R)}$$

This is analogous to the well-known transformation from transmitted light T to extinction E. Extinction is equivalent to the optical density in quantitative microscopy.

$$E = -\log\frac{T}{\max T}$$

Feature Extraction

From each cell nucleus, represented by its mask M and the corresponding region in the fluorescent density image F, numerous quantitative features were calculated describing shape, photometric, and textural properties. The latter are understood as properties of the arrangement of fluorescent particles, which in this case is DNA, visualized by Hoechst 33528. These features are described in detail elsewhere [Rodenacker and Bengtsson, 2003] (Fig. 7). For classification, selected features are briefly described in Tables 6 and 7. They are illustrated by image sequences showing the changing feature value with appropriate cell images.

Statistics and Classification

All statistical evaluations were completed using SAS (SAS Institute, Inc., Cary, NC) and BMDP (Statistical Software, Inc., Los Angeles, CA) program packages. All cells from specimens belonging to the same experimental conditions were pooled and stepwise linear discriminant analysis was applied. From the whole feature set only those features were used in the selection steps that were considered independent of possible global acquisition influences such as relative features and which were univariate significant. Typically, features measuring area or total fluorescent intensity were only used after normalization, for example, particle area divided by nuclear area. Due to the small number of cells, only up to seven (three-class) or six (two-class) features respectively were stepwise selected on the basis of F-statistics to avoid over fitting. The value for the first chosen feature is univariate whereas the following F-values are multivariate reflecting the impact of results after using this feature together with the already selected features. The classification matrices show the results of the hold-one-out (jackknifed) method because no test set was available. All statistical evaluations were done at the 95% confidence level. For display of the three-class discrimination, the canonical variables are used which are linear combinations of the selected features. Linear discriminant analysis results in the so called discriminant function defined by a $((n-1)\text{-classes} \times \text{m-feature})$ matrix D. The canonical variables *CAN* are than defined as

$$CAN = D \cdot \begin{Bmatrix} feature_1 \\ \cdots \\ feature_n \end{Bmatrix}$$

This is the product of the discriminant matrix D and the selected features. This is a method to project the observations for visualization.

RESULTS

Gene Expression and Protein Levels in Microgravity

We analyzed induction of 24 osteoblast genes using linear semi-quantitative RT-PCR. We found reduced gene expression in 10 of these genes; no change in 9 of the genes and copy number was too low to measure in the

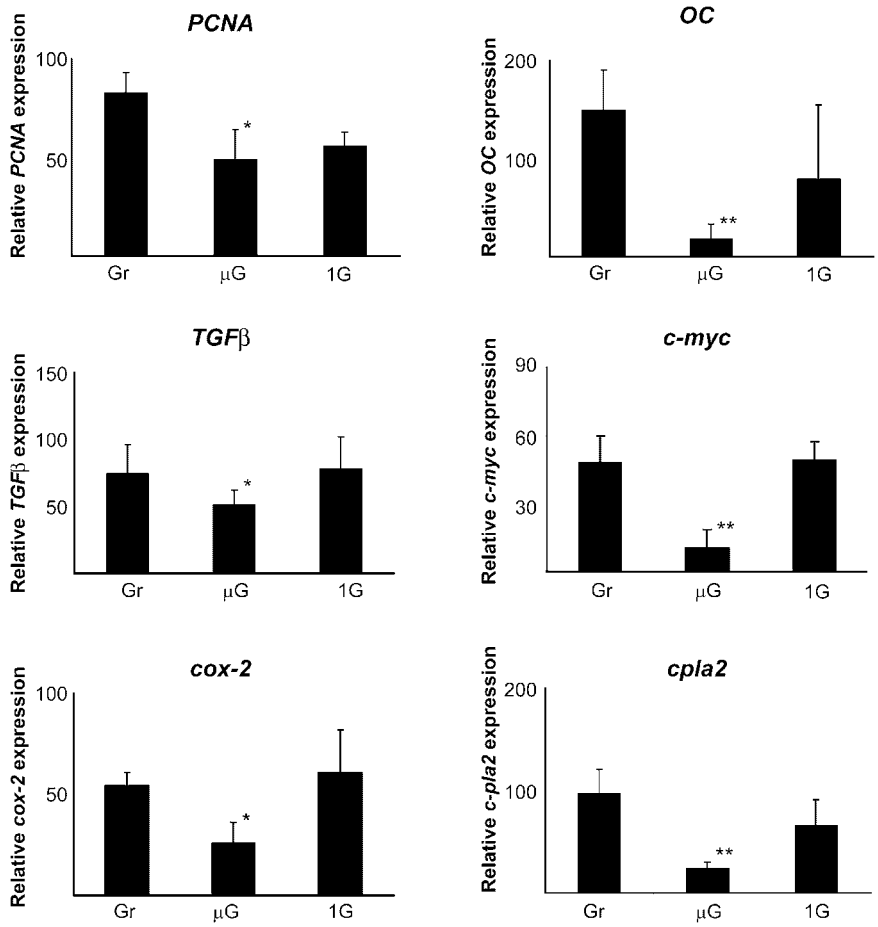

Fig. 2. Analysis of gene expression at 3 h under 1 g flight, μg flight, and ground. N = 4, significance between 1 g and μg levels: $P < 0.001$, significance in ground and μg levels: $P < 0.01$ (bars denotes ± SD).

remaining genes examined. Osteoblasts were activated during space flight in μg with and without a 1 g field and results compared to gr samples. Induction of *PCNA*, *TGFβ*, *cox-2*, *cpla2*, *osteocalcin*, *c-myc*, *fgf-2*, *bcl2*, and *bax* were significantly depressed in μg when compared to gr (Figs. 2 and 3). Artificial onboard gravity was able to normalize the induction of *c-myc*, *cox-2*, *TGFβ*, *fgf-2*, *bax*, and *bcl2* as well as FGF-2 protein synthesis in spaceflight samples.

There was no change in quiescent osteoblast PGE_2 levels (gr 415 ± 163 vs. μg 453 ± 189). Even though the cox-2 message was reduced at 24 h, the PGE_2 levels were high. However, in-flight at 24 h, both the 1 g and the μg samples had a significant rise in PGE_2 levels: 1 g $6{,}065 \pm 870$ and μg $6{,}959 \pm 1132$ versus gr $3{,}904 \pm 1673$ ($P < 0.005$).

Since it has been previously demonstrated that a lack of mitogen causes elongation of nuclei [Foote et al., 1996], we measured endogenous levels of cellular *fgf*-2 message and protein in these microgravity grown samples. In our studies, we found that the *fgf-2* message induction was depressed 24 h after activation (Fig. 3). Moreover, when the cellular protein levels were measured in these cells, we found that *FGF*-2 protein synthesis was also significantly reduced in μg flight, however, the presence of artificial gravity in-flight increased the ability of the cells to synthesize *fgf*-2 (Fig. 3) 24 h after serum activation. Finally, changes in *bcl2* message (Fig. 3) induction parallel that of *fgf*-2 message. The *bcl2* message was significantly decreased in microgravity compared to ground and 1 g samples.

Three-Class Case

This results in the most discriminative features P2A, HETERO, GCV, RHA, RHUA, NR1, and HLM3. A short description of the features selected is given in Tables 6 and 7. Cell nuclei

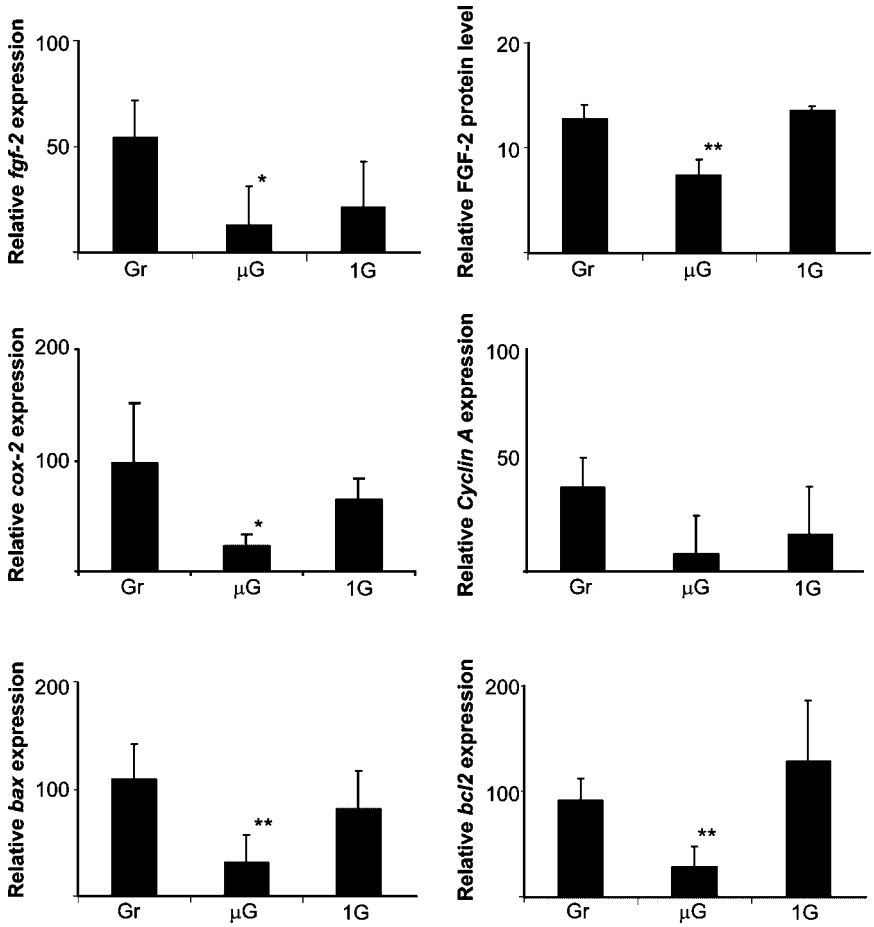

Fig. 3. Analysis of gene expression at 24 h under 1 g flight, μg flight, and ground. N = 4, significance between 1 g and μg levels: $P < 0.001$, significance in ground and μg levels: $P < 0.01$ (bars denotes ± SD).

show clear differences in shape and texture. The first selected feature (P2A) is shape, remaining features are all texture related. Variation of P2A is based on the deviation from circularity to ellipticity. Further differences are reflected by several features sensitive to the different arrangement of bright fluorescent particles (HETERO) inside the darker nucleus surrounding and the less pronounced change between background inside the nucleus and bright particle (GCV).

The classification result is listed in Table 3 and illustrated in Figure 8 using the 1st and 2nd canonical variables (CAN1, CAN2) with the class discrimination lines. Using three-class discrimination analysis, it is clear that the gr and μg cell

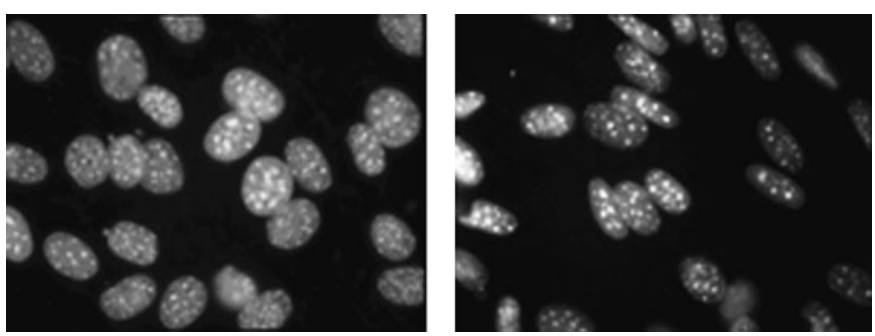

Fig. 4. Original fluorescence image (gr) (left), μg (right).

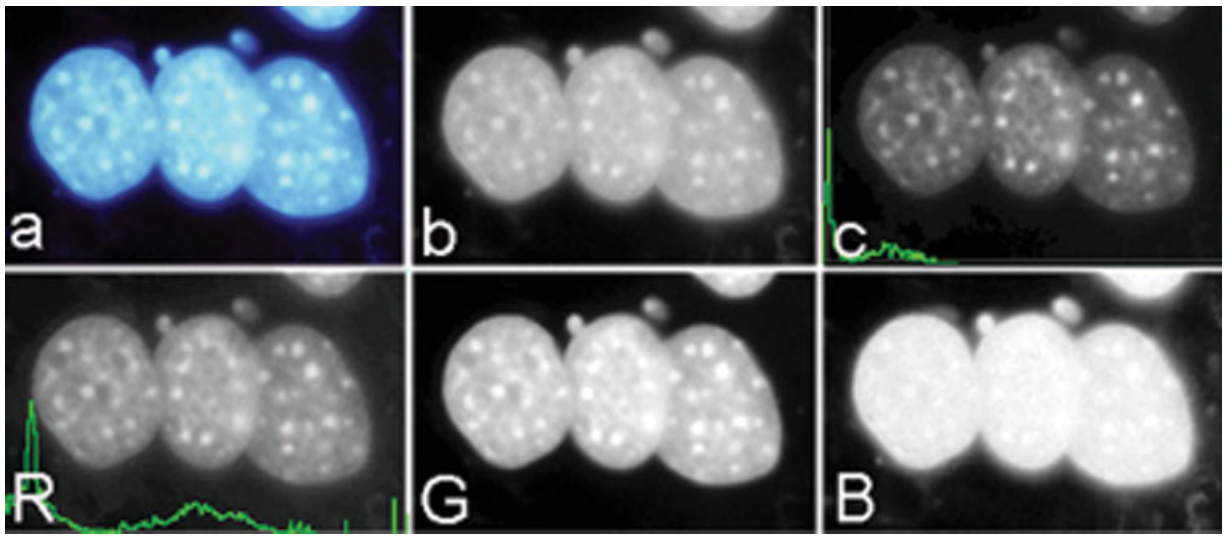

Fig. 5. Effect of different filters on discrimination of features (**a**) original fluorescence image, (**b**) light intensity image, (**c**) fluorescent intensity *F* from RED channel with frequency distribution, (**R**) RED with frequency distribution, (**G**) GREEN, and (**B**) BLUE intensity channel. (Color figure can be viewed in the online issue, which is available at www.interscience.wiley.com.)

populations are significantly different from one another. The first canonical variable CAN1 alone permits a nearly complete discrimination at about CAN1 = 0.8 of the μg cells from the others (see Fig. 8). A sequence of cell images is displayed in Figure 9 using the first canonical variable as order criteria. Note the change of particle structure from left to right.

Two-Class Cases

They were analyzed to find out more about the changes from one experimental condition to another in terms of most selective features.

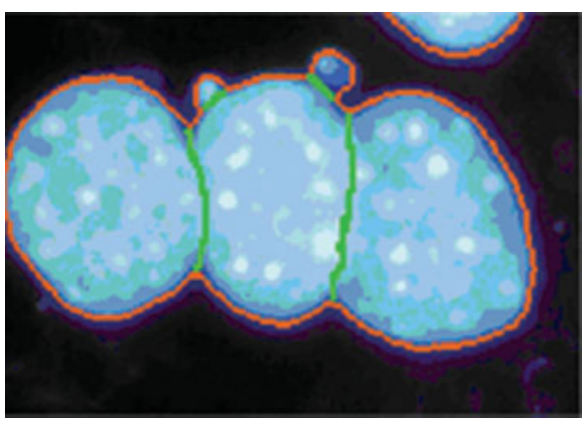

Fig. 6. Segmentation with mask M_r by threshold (red) and manual cutting lines (green). (Color figure can be viewed in the online issue, which is available at www.interscience.wiley.com.)

From ground (gr) to 1 g (in-flight) (Table 4): The selected features HETERO, ELNENL, RHA, and NR4 represent pure textural changes.

From 1 g (in-flight) to μg (Table 5a): The sequence of selected features starts with P2A, a shape factor showing the influence of gravity on growth form, followed by texture features HLM3 and RHUA.

From ground (gr) to μg (Table 5b): For completeness the direct transition from ground (GR) to μg is also outlined. Chosen features are HETERO, RHUA, and RATIO. The first two are pure textural and the last is a shape feature similar to P2A.

The two-class discrimination analysis provided a comparable result with the heterogeneity of nuclear texture (HETERO) showing the greatest difference between gr and μg (correct class 94.7%). A similar difference, with a lower correlation was observed for 1 g and μg (correct class 86.4%). Furthermore, the 1 g cells have very similar morphology to the ground cells (correct class 78.7%). In other words, the ground and 1 g samples are more similar to each other than they are to μg cells. The morphological deviation of μg cells may be due to the influence of gravity on the arrangement of nuclear particles as a result of altered gene expression. All other selected features (HLM3, RHUA, NR2, NC9) except the last are features of particle

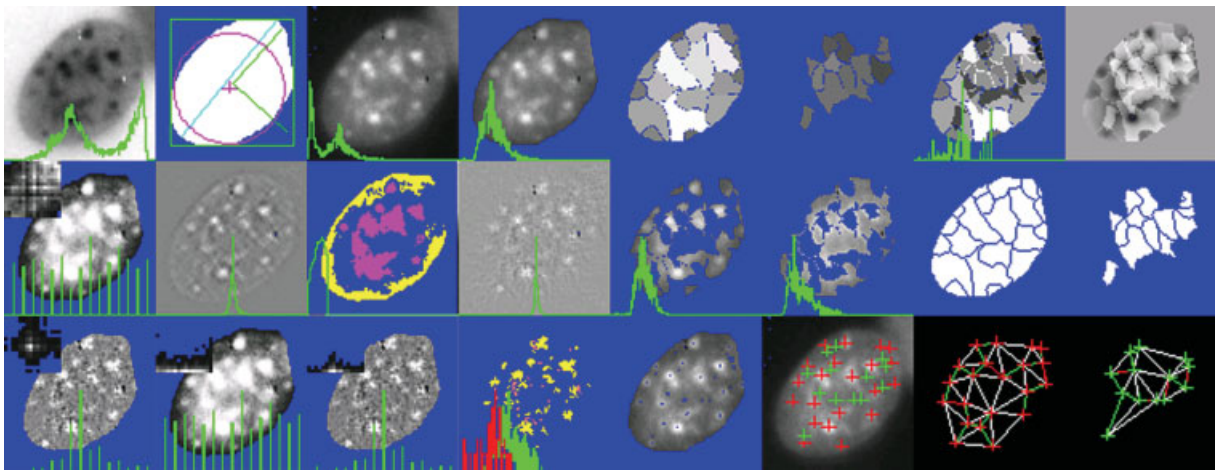

Fig. 7. Illustrations of feature extraction for one nucleus.

arrangement. RATIO reflects an additional shape influence.

DISCUSSION

Combating space osteoporosis is a key factor in planning long-range space missions of greater than 6 months. In order to understand underlying cellular mechanisms of disuse osteoporosis, osteoblasts were grown in μg and 1 g on the Space Shuttle and were analyzed for changes in gene expression and morphology after growth stimulation. We noted visual differences in nuclear shape in cells growth in μg. Since changes in autocrine, growth, cytoskeletal, and transcription factors may be important in osteoblast physiology in spaceflight [Cubano and Lewis, 2000; Goodwin et al., 2000], we analyzed 24 osteoblast genes under μg, 1 g, and gr conditions. Of the genes with significantly altered expression, there were four cell cycle related, one osteoblast specific, two immediate early, and two growth factor genes reduced at one or both of the timepoints. Many genes had no significant change in message level, these included 18 S, H4 histone, fibronectin, β-actin, cyclophilin, and prostaglandin E_2 receptor 1 (EP1). In contrast, there were nine genes that had a significant reduction in message induction in μg, these included *cox-2*, *cpla2*, *PCNA*, *bcl2*, *bax*, *c-myc*, *TGFβ*, *OC*, and *fgf-2* suggesting a change in anabolic response in the absence of gravity.

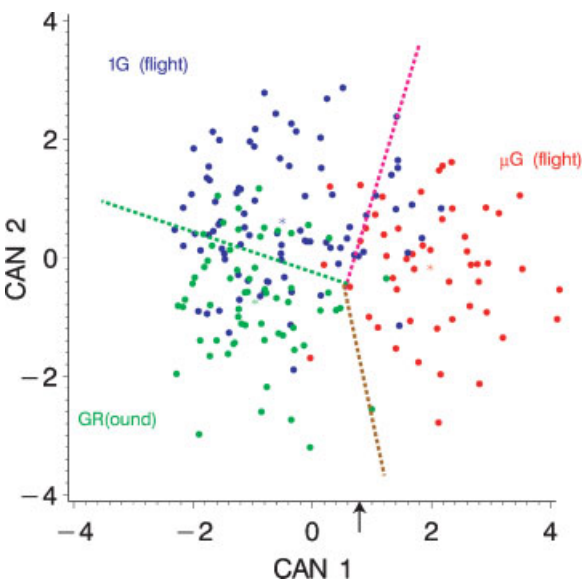

Fig. 8. Three-class discrimination result using the 1st and 2nd canonical variables with discrimination lines between respective classes.

Of particular interest was the reduction in *cox-2* message in the presence of high levels of PGE_2. Cox-2 is a key enzyme in the maintenance of bone in response to stress and exercise [Forwood, 1996; Forwood et al., 1998]. Moreover, cox-2 is a feed-forward enzyme, which is induced by its own product, PGE_2 [Pilbeam et al., 1995]. In μg, this feed-forward regulation becomes uncoupled, with PGE_2 levels significantly increased in both the 1 g ($P < 0.05$) and the μg ($P < 0.001$) osteoblasts when compared to gr controls. The underlying mechanism for this uncoupling is currently under study using modeled μg and understanding the loss of feed-forward induction of cox-2 at the cellular level may help us understand the loss of bone in astronauts.

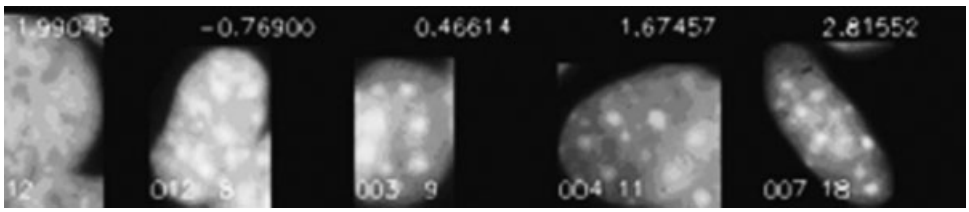

Fig. 9. Transition of gr, 1 g cells to μg cells ordered by the first canonical variable CAN1 from the three-class discrimination (see Fig. 6) in the interval CAN1 $\in [-2,3]$. Notice the changes of the bright 'particle' structures from left to right. The corresponding CAN1 values are outlined in the upper image regions.

Messenger RNA and protein content of FGF-2, an important transcription and autocrine growth factor in bone [Stachowiak et al., 1994; Keresztes and Boonstra, 1999], was depressed in the μg samples. There are at least three isoforms of *fgf-2*, both the PKA and PKC signaling pathways act synergistically to stimulate synthesis of each of these forms [Stachowiak et al., 1994]. PKA results in more *fgf-2* being associated with the intracellular (transcription factor) pathway, while PKC causes accumulation in the cytoplasm and secretion [Stachowiak et al., 1994]. We found that after 24 h in microgravity, the cells had a significant fivefold decrease in both FGF-2 protein and message when compared to gr samples. This corresponds well with the gene chip data of Hammond et al. who reported a sixfold decrease in mRNA signal for *fgf-2* message and its receptor in rat kidney cells grown on the Space shuttle for 6 days [Hammond et al., 2000]. Since *fgf-2* is known to regulate *bcl2* in small lung cancer cells, we analyzed message for *bcl2* and found that its expression was also lowered in osteoblasts 24 h after activation in μg. The role of the cytoskeleton in growth and its relationship to cell cycle and the anabolic MAPK signal transduction pathway is being actively investigated in this laboratory. We have recently reported that gravity strain can stimulate osteoblast cytoskeleton and growth through a MAPK mechanism, most likely a PKA pathway [Hatton et al., 2003]. The PKA pathway might also be effected in microgravity since it is known to mediate induction of *fgf-2* [Stachowiak et al., 1994] and promote growth in osteoblasts [Barry et al., 1999; Fitzgerald et al., 2000].

In coordination with the changes in induction of gene expression, the cells demonstrated a significant difference in shape (roundish/elliptic), nuclear structure, and texture (less/more bright particles, less/more densely packed, less/more contrasted) when exposed to μg. Mathematical analysis of morphology demonstrated a significant differentiation of single cells grown under varying gravity conditions. To apply an a-posteriori classification scheme to discriminate microgravity conditions the number of specimens has to be increased. The cause of the elongation of nuclei and elongation of cytoskeleton in microgravity is not known, although Rijken et al. noted cell shape changes previously [de Groot et al., 1991]. It is possible that it is a result of a microgravity-induced inhibition of anabolic stimulation. The only example we found of similar nuclear elongation was caused by limiting cell access to mitogens [Wang and Walsh, 1996].

Studies by Wang and Walsh [Foote et al., 1996] demonstrated that when myocytes undergo growth factor withdrawal, a portion of the cells form elongated nuclei, a shape much like those seen in our spaceflight samples in μg. The classification results additionally show that 1 g in-flight cells differ only little from gr although the shape is slightly changed. Table 4 shows that

TABLE IV. Two-Class Jackknifed Classification Results (gr ~ 1 g) With the Three Most Important Features and Their Corresponding *F*-Values (see Also Tables VI and VII)

	%	gr	1 g	Feature	*F*-value
gr	71.6	55	7	HETERO	20.3
1 g	88.7	25	63	ELNENL	16.5
Total	78.7			RHA	10.6

TABLE VA. Two-Class Jackknifed Classification Results (1 g ~ μg) With the Three Most Important Features and Their Corresponding *F*-Values (see Also Tables VI and VII)

	%	μg	1 g	Feature	*F*-value
μg	90.4	47	5	P2A	69.5
1 g	81.8	16	72	HLM3	32.6
Total	85.0			RHUA	11.6

TABLE VB. Two-Class Jackknifed Classification Results (gr ~ μg) With the Three Most Important Features and Their Corresponding *F*-Values (see Also Table VII and VIII)

	%	gr	μg	Feature	*F*-value
gr	96.2	58	4	HETERO	98.9
μg	93.5	2	50	RHUA	43.2
Total	94.7			RATIO	30.1

only texture features with relatively low F-values allow a 78.7% correct classification. Differences are possibly due to the 19 h storage of the quiescent osteoblasts in μg in the Type I containers prior to serum activation and being placed in a 1 g environment. In addition, Wang and Walsh [1996] reported that myocytes had a spindle-shaped elongation of cells, which accompanied the elongation of the nucleus. Our studies here as well as our previous studies in space flight [Fitzgerald and Hughes-Fulford, 1996] suggest that there is an elongation of the nucleus in cells grown in microgravity. These findings are supported by the observations of Guignandon et al. [1995] who also observed that intermittent effect of gravity causes flight-induced shape changes that included focal contact plaque reorganization. When cells were blocked in G2/M with nocodazole the flight-induced decrease in adhesion was ameliorated, suggesting that microtubules play a role in gravity-induced changes of the nuclear structure. Results from several investigators suggest that the actin cytoskeleton is a necessary component of the cell cycle, especially needed for transition from G1-S phase and for anchorage dependent DNA synthesis [Carvalho et al., 1998; Pavalko et al., 1998]. Restrictions to the cytoskeleton formation inhibit growth [Bohmer et al., 1996; Brighton et al., 1996; Hughes-Fulford and Lewis, 1996;

TABLE VI. Most Important Features From Three-Class Discrimination With Image Sequences of Increasing Feature Values

$$\mathrm{P2A} = \frac{\mathrm{P}^2}{\mathrm{A} \times 4\pi}$$

Shape factor of nucleus mask; P, perimeter; A, area

$$\mathrm{HETERO} = \frac{\mathrm{A} - \#\mathrm{pels} \in [\mathrm{M1} \pm 20\%]}{\mathrm{A}}$$

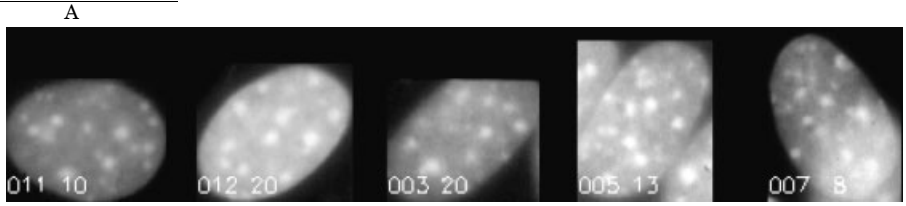

$$\mathrm{GCV} = \frac{\mathrm{GM2}}{\mathrm{GM1}}$$

Coefficient of variation of gradient transformed image; GM1, mean gradient; GM2, SD gradient

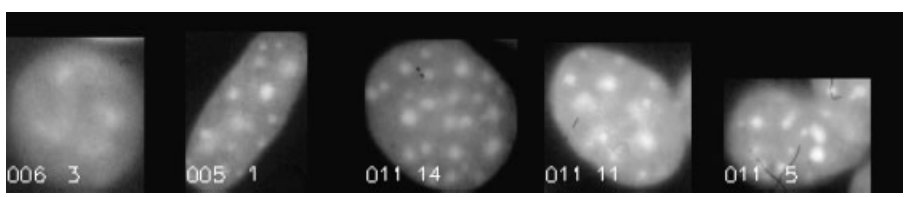

$$\mathrm{RHA} = \frac{\mathrm{HM1} \cdot \mathrm{HA}}{\mathrm{M1} \cdot \mathrm{A}}$$

Ratio of total particle fluorescent intensity and total fluorescent; HM1, fluorescent, intensity of bright particles; HA, area of bright particles, M1, A s. a.

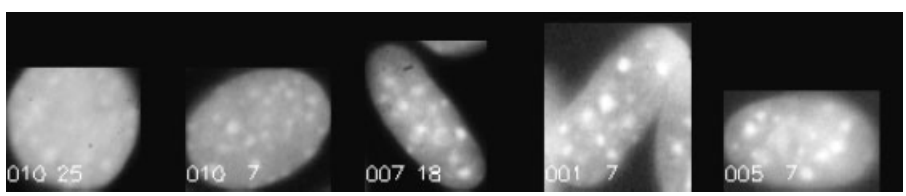

TABLE VII. Most Important Features From Two-Class Discriminations With Image Sequences of Increasing Feature Values

$$\mathrm{RHUA} = \frac{\mathrm{HUM1} \times \mathrm{HUA}}{\mathrm{M1} \times \mathrm{A}}$$

Ratio of total bright particle zone fluorescent intensity and total fluorescent intensity; HUM1, mean fluorescent intensity of bright particle zone; HUA, area of bright particle zone, M1, A s. a.

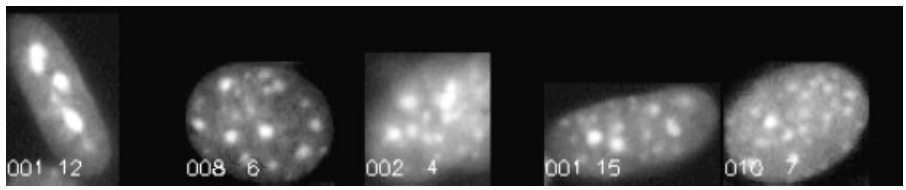

HLM3

Skewness of fluorescent intensity of dark (non-) particle zones

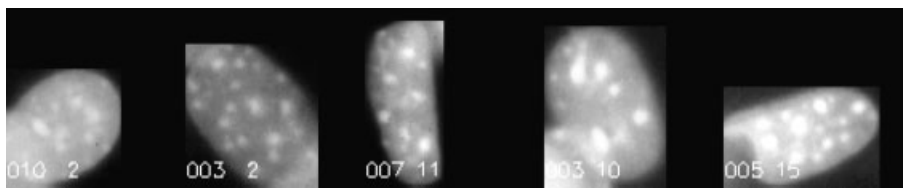

$$\mathrm{RATIO} = \frac{\mathrm{RAD}}{\mathrm{MXDU}}$$

RAD, maximum inscribable circle; MXDU, maximum horizontal and vertical extension

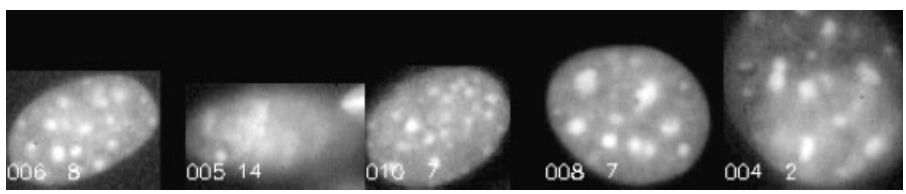

ELNENL

Graph feature: total length of nearest neighbor graph of dark particle zone centroids

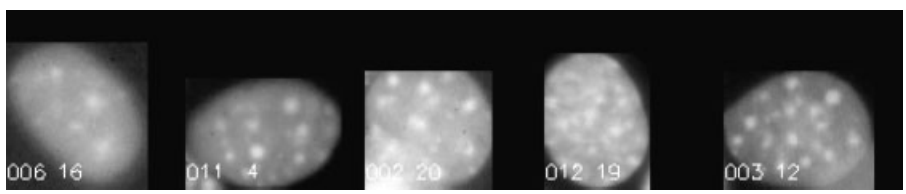

Rosenberg, 2003] and can induce differentiation [Ingber et al., 1995; Hii et al., 1998; Dike et al., 1999]. A review of osteoblast signaling also suggest that key pathways may be linked to stress and related gravity forces [Hughes-Fulford, 2004]. The obvious changes in nuclear morphology in microgravity conditions may be a key component in regulation of growth and differentiation and may further link cytoskeletal anomalies in space-flown cells to nuclear function suggesting that the cytoskeleton is an important component of osteoblast physiology in microgravity and on earth.

Beside the visual recognizability and mathematically measurable shape changes of the nuclei, the deviations of nuclear structure suggest that cell functions are changed under microgravity. Analogous to nuclear texture changes during cell cycle (nearly no texture in synthesis periods, increased texture in periods of standstill like G0/G1), these cells show a certain cell cycle quiescence, suggesting a lag in

the anabolic signaling processes. Most likely cell cycle progression slows in the microgravity environment since the size of most of the microgravity cells does not show a large G2 (doubling) size. The fixed cells are only 0.4-μm thick so the diameter is a good measure of DNA in cells that are anchored (not rounded in preparation for mitosis or coming out of mitosis).

In this study, sera activation failed to fully stimulate synthesis of *cox-2*, *cpla2*, *c-myc*, *TGFβ*, *OC*, *PCNA*, *bcl2*, and *fgf-2* message as well as FGF-2 protein in μg, suggesting that gravity is needed for some early anabolic signals. Conversely, it is of interest to note that *cox-2*, *OC*, and *fgf-2* are induced by mechanical stress [Hatton et al., 2003] and therefore their downregulation in the absence of stress during spaceflight suggests an earthbound mechanism for these anabolic responses. It is likely that cellular studies of the osteoblast in microgravity will provide new mechanistic models and pharmaceutical targets for disuse osteoporosis in astronauts and the elderly. Moreover, since all terrestrial organisms have evolved in a 1 g environment, these studies add to our understanding of the effect of earth's gravity on fundamental biological laws underlying life itself.

ACKNOWLEDGMENTS

We thank Janice Voorsluys and Theresa Marsh for their thoughtful comments and review of this manuscript. The authors thank the following members of the Laboratory of Cell Growth who assisted in preparation of this manuscript; Sina Sayyah, Emily Sear, Yvonne Ha, and Janice Voorsluys. This research was supported in part by NASA grants NAG-2-1086, NAG-2-1286, NCC-2-136 and the Department of Veterans Affairs Research Service Merit Review in support of MHF.

REFERENCES

Barry OP, Kazanietz MG, Pratico D, FitzGerald GA. 1999. Arachidonic acid in platelet microparticles upregulates cyclooxygenase-2-dependent prostaglandin formation via a protein kinase C/mitogen-activated protein kinase-dependent pathway. J Biol Chem 274:7545–7556.

Bohmer RM, Scharf E, Assoian RK. 1996. Cytoskeletal integrity is required throughout the mitogen stimulation phase of the cell cycle and mediates the anchorage-dependent expression of cyclin D1. Mol Biol Cell 7:101–111.

Brighton CT, Fisher JR, Jr, Levine SE, Corsetti JR, Reilly T, Landsman AS, Williams JL, Thibault LE. 1996. The biochemical pathway mediating the proliferative response of bone cells to a mechanical stimulus. J Bone Jt Surg Am 78:1337–1347.

Canalis E, McCarthy TL, Centrella M. 1991. Growth factors and cytokines in bone cell metabolism. Annu Rev Med 42:17–24.

Carmeliet G, Nys G, Stockmans I, Bouillon R. 1998. Gene expression related to the differentiation of osteoblastic cells is altered by microgravity. Bone 22:139S–143S.

Carvalho RS, Schaffer JL, Gerstenfeld LC. 1998. Osteoblasts induce osteopontin expression in response to attachment on fibronectin: Demonstration of a common role for integrin receptors in the signal transduction processes of cell attachment and mechanical stimulation. J Cell Biochem 70:376–390.

Coffin JD, Florkiewicz RZ, Neumann J, Mort-Hopkins T, Dorn GW 2nd, Lightfoot P, German R, Howles PN, Kier A, O'Toole BA, Sasse J, Gonzalez AM, Baird A, Doetschmon T. 1995. Abnormal bone growth and selective translational regulation in basic fibroblast growth factor (FGF-2) transgenic mice. Mol Biol Cell 6:1861–1873.

Cubano LA, Lewis ML. 2000. Fas/APO-1 protein is increased in spaceflown lymphocytes (Jurkat). Exp Gerontol 35:389–400.

de Groot RP, Rijken PJ, den Hertog J, Boonstra J, Verkleij AJ, de Laat SW, Kruijer W. 1990. Microgravity decreases c-fos induction and serum response element activity. J Cell Sci 97:33–38.

de Groot RP, Rijken PJ, Boonstra J, Verkleij AJ, de Laat SW, Kruijer W. 1991. Epidermal growth factor-induced expression of c-fos is influenced by altered gravity conditions. Aviat Space Environ Med 62:37–40.

Debnath J, Chamorro M, Czar MJ, Schaeffer EM, Lenardo MJ, Varmus HE, Schwartzberg PL. 1999. rlk/TXK encodes two forms of a novel cysteine string tyrosine kinase activated by Src family kinases. Mol Cell Biol 19:1498–1507.

Dike LE, Chen CS, Mrksich M, Tien J, Whitesides GM, Ingber DE. 1999. Geometric control of switching between growth, apoptosis, and differentiation during angiogenesis using micropatterned substrates. In Vitro Cell Dev Biol Anim 35:441–448.

Fitzgerald J, Hughes-Fulford M. 1996. Gravitational loading of a simulated launch alters mRNA expression in osteoblasts. Exp Cell Res 228:168–171.

Fitzgerald J, Hughes-Fulford M. 1999. Mechanically induced c-fos expression is mediated by cAMP in MC3T3-E1 osteoblasts. Faseb J 13:553–557.

Fitzgerald J, Dietz TJ, Hughes-Fulford M. 2000. Prostaglandin E2-induced up-regulation of c-fos messenger ribonucleic acid is primarily mediated by 3′,5′-cyclic adenosine monophosphate in MC3T3-E1 osteoblasts. Endocrinology 141:291–298.

Foote LC, Schneider TJ, Fischer GM, Wang JK, Rasmussen B, Campbell KA, Lynch DH, Ju ST, Marshak-Rothstein A, Rothstein TL. 1996. Intracellular signaling for inducible antigen receptor-mediated Fas resistance in B cells. J Immunol 157:1878–1885.

Forwood MR. 1996. Inducible cyclo-oxygenase (COX-2) mediates the induction of bone formation by mechanical loading in vivo. J Bone Miner Res 11:1688–1693.

Forwood MR, Kelly WL, Worth NF. 1998. Localisation of prostaglandin endoperoxide H synthase (PGHS)-1 and

PGHS-2 in bone following mechanical loading in vivo. Anat Rec 252:580–586.
Goodwin TJ, Coate-Li L, Linnehan RM, Hammond TG. 2000. Selected contribution: A three-dimensional model for assessment of in vitro toxicity in balaena mysticetus renal tissue. J Appl Physiol 89:2508–2517.
Granet C, Boutahar N, Vico L, Alexandre C, Lafage-Proust MH. 2001. MAPK and SRC-kinases control EGR-1 and NF-kappa B inductions by changes in mechanical environment in osteoblasts. Biochem Biophys Res Commun 284:622–631.
Guignandon A, Vico L, Alexandre C, Lafage-Proust MH. 1995. Shape changes of osteoblastic cells under gravitational variations during parabolic flight—Relationship with PGE2 synthesis. Cell Struct Funct 20:369–375.
Hammond TG, Benes E, O'Reilly KC, Wolf DA, Linnehan RM, Taher A, Kaysen JH, Allen PL, Goodwin TJ. 2000. Mechanical culture conditions effect gene expression: Gravity-induced changes on the space shuttle. Physiol Genomics 3:163–173.
Hatton JP, Pooran M, Li CF, Luzzio C, Hughes-Fulford M. 2003. A short pulse of mechanical force induces gene expression and growth in MC3T3-E1 osteoblasts via an ERK 1/2 pathway. J Bone Miner Res 18:58–66.
Hii CS, Huang ZH, Bilney A, Costabile M, Murray AW, Rathjen DA, Der CJ, Ferrante A. 1998. Stimulation of p38 phosphorylation and activity by arachidonic acid in HeLa cells, HL60 promyelocytic leukemic cells, and human neutrophils. Evidence for cell type-specific activation of mitogen-activated protein kinases. J Biol Chem 273:19277–19282.
Hiramatsu M, Ikeda E, Kashimata M, Minami N, Kodama H, Sudo H, Kumegawa M. 1983. Effect of dibutyryl cyclic AMP on collagen synthesis in a clonal osteoblast-like cell line derived from newborn mouse calvaria. J Biochem (Tokyo) 94:1353–1358.
Hughes-Fulford M. 2004. Signal transduction and mechanical stress. Sci STKE 2004:RE12.
Hughes-Fulford M, Lewis ML. 1996. Effects of microgravity on osteoblast growth activation. Exp Cell Res 224:103–109.
Hughes-Fulford M, Appel R, Kumegawa M, Schmidt J. 1992. Effect of dexamethasone on proliferating osteoblasts: Inhibition of prostaglandin E2 synthesis, DNA synthesis, and alterations in actin cytoskeleton. Exp Cell Res 203:150–156.
Ingber DE, Prusty D, Sun Z, Betensky H, Wang N. 1995. Cell shape, cytoskeletal mechanics, and cell cycle control in angiogenesis. J Biomech 28:1471–1484.
Keresztes M, Boonstra J. 1999. Import(ance) of growth factors in(to) the nucleus. J Cell Biol 145:421–424.
Landis WJ, Hodgens KJ, Block D, Toma CD, Gerstenfeld LC. 2000. Spaceflight effects on cultured embryonic chick bone cells. J Bone Miner Res 15:1099–1112.
Lewis ML, Cubano LA, Zhao B, Dinh HK, Pabalan JG, Piepmeier EH, Bowman PD. 2001. cDNA microarray reveals altered cytoskeletal gene expression in space-flown leukemic T lymphocytes (Jurkat). Faseb J 15: 1783–1785.
Marie PJ, Jones D, Vico L, Zallone A, Hinsenkamp M, Cancedda R. 2000. Osteobiology, strain, and microgravity: Part I. Studies at the cellular level. Calcif Tissue Int 67:2–9.
Nicogossian A, Huntoon C, Pool S. 1989. Space physiology and medicine. Philadephia: Lea and Febiger.
Pavalko FM, Chen NX, Turner CH, Burr DB, Atkinson S, Hsieh YF, Qiu J, Duncan RL. 1998. Fluid shear-induced mechanical signaling in MC3T3-E1 osteoblasts requires cytoskeleton-integrin interactions. Am J Physiol 275: C1591–C1601.
Pilbeam CC, Raisz LG, Voznesensky O, Alander CB, Delman BN, Kawaguchi H. 1995. Autoregulation of inducible prostaglandin G/H synthase in osteoblastic cells by prostaglandins. J Bone Miner Res 10:406–414.
Rodenacker K, Bengtsson E. 2003. A feature set for cytometry on digitized microscopic images. Anal Cell Pathol 25:1–36.
Rosenberg N. 2003. The role of the cytoskeleton in mechanotransduction in human osteoblast-like cells. Hum Exp Toxicol 22:271–274.
Stachowiak MK, Moffett J, Joy A, Puchacz E, Florkiewicz R, Stachowiak EK. 1994. Regulation of bFGF gene expression and subcellular distribution of bFGF protein in adrenal medullary cells. J Cell Biol 127:203–223.
Vico L, Collet P, Guignandon A, Lafage-Proust MH, Thomas T, Rehaillia M, Alexandre C. 2000. Effects of long-term microgravity exposure on cancellous and cortical weight-bearing bones of cosmonauts. Lancet 355:1607–1611.
Wang J, Walsh K. 1996. Resistance to apoptosis conferred by Cdk inhibitors during myocyte differentiation. Science 273:359–361.
Wronski TJ, Morey ER. 1983. Effect of spaceflight on periosteal bone formation in rats. Am J Physiol 244: R305–R309.
Young IT, Verbeek PW, Mayall BH. 1986. Characterization of chromatin distribution in cell nuclei. Cytometry 7: 467–474.